Probing the dynamics of highly excited toluene in the fs timescale

Journal:	*Physical Chemistry Chemical Physics*
Manuscript ID	CP-ART-07-2015-004346.R1
Article Type:	Paper
Date Submitted by the Author:	06-Oct-2015
Complete List of Authors:	Kosmidis, Constantine; University of Ioannina, Physics Papadopoulou, Christina; University of Ioannina, Physics Kaziannis, Spiridon; University of Ioannina, Physics

Probing the dynamics of highly excited toluene in the fs timescale

C. C. Papadopoulou, S. Kaziannis, C. Kosmidis*

Department of Physics, Atomic and Molecular Physics Laboratory,
University of Ioannina, University Campus, Ioannina GR-45110, Greece
*Author for correspondence: kkosmid@uoi.gr

Abstract

Investigation of the dynamics of toluene-h_8 ($C_6H_5CH_3$), toluene-d_8 ($C_6D_5CD_3$) and toluene-α,α,α-d_3 ($C_6H_5CD_3$) has been performed utilizing the VUV pump-IR probe technique in the fs timescale. Using the 5th harmonic (~160 nm) of a Ti:Sapphire laser as the pump beam, two superimposed electronic states, the valence S_3 and the Rydberg 4p, were excited by one-photon absorption, followed by ionization and dissociation induced by the probe beam (800 nm).

Analysis of the transient signal of the parent (P^+) and fragment ions ($[P-H]^+$ or $[P-D]^+$) implies the existence of two different relaxation processes: i) from the Rydberg and ii) from the S_3 valence state. Using a rate equation model, the decay times have been determined and comparison between the different isotopologues has been made. Conclusions on the relaxation path, the relative displacements of the potential energy surfaces and the activation energies needed have been drawn from the decay times. The signals corresponding to the fragment ions present a small in amplitude, but nonetheless, unambiguous periodical modulation, which is attributed to out-of-plane bending oscillation, involving also the methyl group.

The dynamics of the H- and D-loss channels has been investigated. Especially for the case of toluene-α,α,α-d_3, where both channels are in operation, it was found that the ratio of the abundance of H/D-loss dissociation reactions decreases as the pump-probe delay time increases.

Introduction

During the past few decades a lot of discussion has been made on the photophysical dynamics of small organic molecules, including substituted aromatic ones. Beyond the fundamental importance of the understanding of their photophysical dynamics, their usage in a broad spectrum of applications has contributed decisively to the great interest on their properties. Among them, toluene ($C_6H_5CH_3$) can be considered as a benchmark molecule, since it is one of the simplest substituted monocyclic aromatic compounds and one of the most extensively used substances in various fields of chemistry. Thus, it has been a matter of study, both theoretically and experimentally, concerning its photophysical and photochemical properties.

Internal conversion (IC), as one of the dominant mechanisms for deactivation of higher to vibrationally excited lower electronic states, has been extensively studied in the cases of benzene[1,2] and some alkyl-substituted derivatives.[2–5] Usually, the cases of the S_2 and S_1 valence excited states were concerned, while the S_3 state is rather challenging case due to its superposition with Rydberg states.[6] Suzuki *et al.*[2] determined a lifetime of ~62 fs for the S_2 state of toluene, while Farmanara *et al.*[5] determined lifetimes of ~50 fs and ~4.3 ps for the S_2 and S_1 electronic states respectively in the case of toluene monomer by investigating the $S_2 \rightarrow S_1 \rightarrow S_0$ process. Their earlier attempt on the investigation of the dynamics of several molecules after excitation at 155 nm[4] resulting in a lifetime of about 100 fs for toluene, but no conclusive assignment of this was made.

The existence of conical intersections in the neutral and the ionic manifold of toluene as well as their influence on the dynamics has been also a matter of theoretical investigation.[7,8] Moreover, in the case of the S_1/S_0 conical intersection, the first excited triplet state T_1 is also degenerate with the two singlet states, leading to intersystem crossing and dissociation apart from internal conversion.[9]

Another process that has attracted the researchers' interest for over four decades is the possibility of isomerization of toluene to a seven-membered ring compound.[10–12] Assiduous studies on this issue by Lifshitz and coworkers using the time-resolved photoinization mass spectrometry (TRIMS) technique were performed in the early 90s.[13–15] They showed that the seven-membered cyclic tropylium fragment ion (Tr^+, $C_7H_7^+$) is generated in the ionic manifold, with the isomerization process taking place prior to H-elimination or *vice versa*. More recently, Lin *et al*. performed pump-probe experiments at 193 nm on isotope labeled-toluene in the nanosecond timescale and showed that this isomerization actually occurs from the neutral molecule too in this long time range.[16]

The present work aims to investigate the dynamics of highly excited toluene and especially to improve our understanding of the processes taking place in the fs timescale following the excitation in the S_3 valence state. For this purpose, we employed the VUV pump-IR probe technique in the fs timescale in combination with time-of-flight mass spectrometry (TOF-MS). We are also interested in exploring isotopic effects on the dynamics and, therefore, two deuterium labeled isotopes of toluene: toluene-d_8 and toluene-α,α,α-d_3 are studied along with the toluene-h_8 molecule. It should be noted that the effect of isotopic substitution in toluene has been also a topic that attracted a lot of interest in the past.[3,17–20] However, to the best of our knowledge the investigation of the dynamics of these primary dissociation channels, i.e. the H- (or D-) loss, is attempted in the present work for the first time in the literature.

Experimental details

In the present study, VUV pump-IR probe mass spectroscopy was employed. The fundamental frequency of a Ti:Sapphire fs pulsed laser (Coherent Micra and Legend Elite Duo USX, central wavelength at 800 nm, pulse duration 30 fs, ~60 nm bandwidth, p-polarization, repetition rate 1 kHz) was used. The main part of the experimental setup consisted of a Mach-Zehnder type interferometer. In the first arm the fundamental beam was focused in a static Ar cell, generating thus odd harmonics.[21,22] The 5th harmonic (~160 nm, pump beam) was isolated with a specially designed mirror. In the second arm the fundamental pulse underwent PC-controlled delay relatively to the pump pulse by entering a moving stage with mirrors. Finally, the two beams were recombined and propagated collinearly towards an Al spherical mirror focusing them on the gas-phase molecular sample (for more details, see supporting information and Scheme 1). The pulse energies on the target were estimated at ~150 nJ and ~1.5 μJ for the pump and the probe pulse respectively. Similar techniques have been used by several researchers in the past.[4,23]

For each temporal scan the definition of zero delay between the pump and probe beams along with a measurement of the response function of the setup was based on the parasitic water signal. According to Trushin *et al.*,[24] the water molecule has a very short-lived electronic excited state at ~160 nm (1.8 fs), that is negligible in our case (where the experimental error is at least 10 fs as will be discussed later) at the determination of the zero delay between the two pulses.

The generated ions were detected by a time-of-flight mass spectrometer (TOF-MS) coupled with Microchannel Plates (MCPs). For each delay step of the probe beam relatively to the pump, a TOF mass spectrum accumulating 10^4 shots was recorded (via a P7888 time-of-flight multiscaler, Fast ComTec) and further processed using a PC. Six or seven consecutive runs under the same conditions with a step of 10 fs were performed for each molecule under study. In order to improve the signal-to-noise ratio, the acquired single-scan measurements are added together, after careful calibration of their time-axis based on the H_2O^+ pump-probe signals.

Toluene-h_8 and toluene-d_8 were obtained with nominal purities 99.5% by Sigma-Aldrich and Deutero GmbH respectively and toluene-α,α,α-d_3 with 98% purity by Santa Cruz Biotechnology. They were used without further treatment except for the degassing by multiple freeze-pump-thaw cycles. The gas-phase sample at room temperature was effusively inserted in the interaction region of the TOF-MS. The background pressure was usually approximately 10^{-7} mbar, while the experiments were performed at a ~$5\text{x}10^{-6}$ mbar pressure.

Results and Discussion

Using the experimental process described above, the mass spectra of the three molecules have been recorded. The intensity of the pump beam was not sufficient to produce detectable ionic signal on its own. Moreover, the intensity of the probe beam was deliberately adjusted to a value where no ionic signal was observed and to minimize the appearance of fragment ions at zero pump/probe delay time too.

1) Toluene-h_8

A typical spectrum of toluene-h_8 resulting from the interaction with both beams at a delay time Δt=44 fs is shown in Fig. 1. Clearly, only the parent P^+ and the fragment [P-

H]$^+$ ions, at m/z=92 and 91 respectively, appear in the mass spectra. The ion peak at m/z=93 corresponds to the parent ions containing a ^{13}C atom.

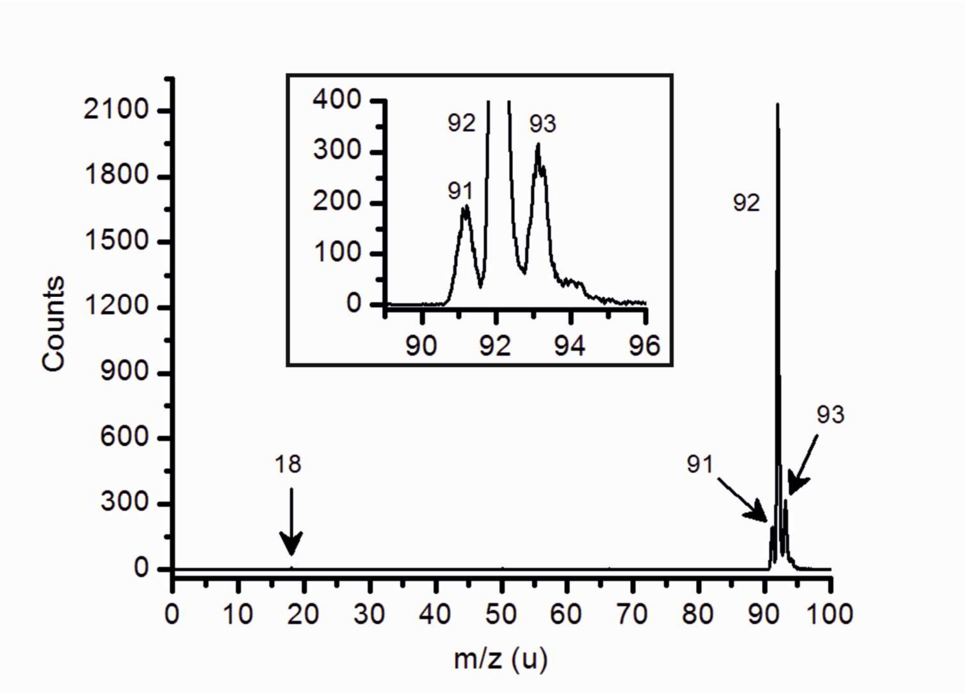

Fig. 1 Time-of-flight mass spectrum at 44 fs delay time. In the inset the peaks of interest around m/z=92 are shown clearly.

In Fig. 2 the dynamics of P$^+$ ($C_7H_8^+$) and [P-H]$^+$ ($C_7H_7^+$) is depicted. The positions of the maxima are also noted. Obviously, the dependence on the time delay of these two ions is not the same. In Scheme 4 of the supporting information, the dynamics is also presented in logarithmic scale (the same applies for the other two molecules).

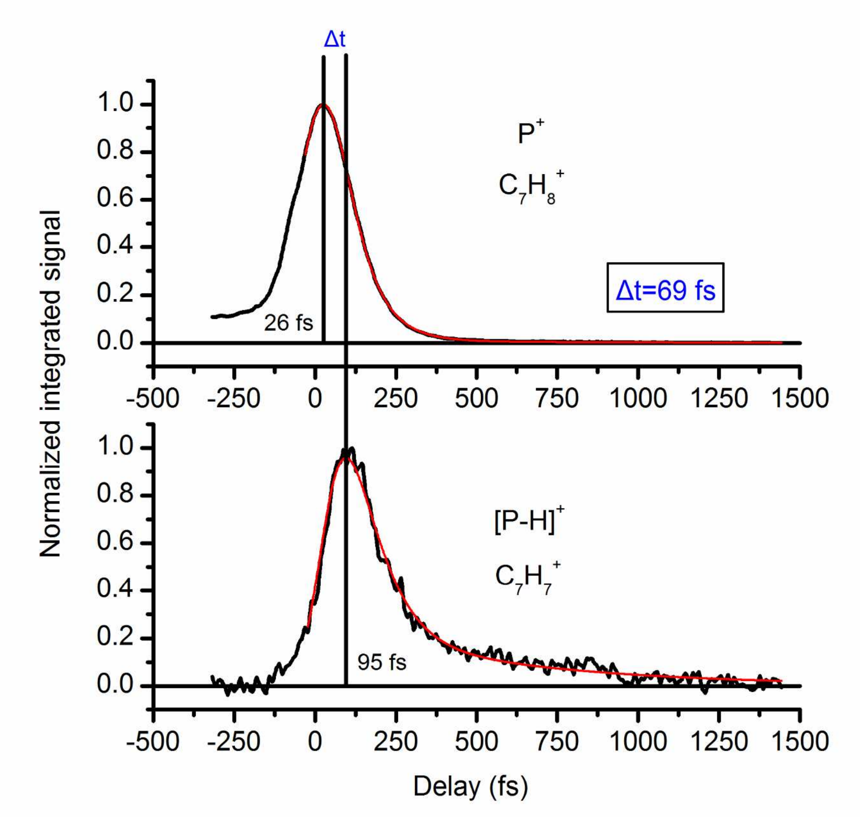

Fig. 2 Normalized sum of six normalized scans for the case of toluene-h_8 (black lines). The fitting with eq. (6) (sup. information, red line) and the peak-signal positions are also shown.

2) Toluene-d_8

The fully deuterated toluene was studied under the same experimental conditions as toluene-h_8. Only two peaks originating from toluene-d_8, i.e. P^+ ($C_7D_8^+$) and $[P\text{-}D]^+$ ($C_7D_7^+$) at m/z=100 and 98 respectively, have been recorded in the TOF mass spectra in agreement with the toluene-h_8 case.

In Fig. 3 the dynamics of these two ions are depicted along with their maxima positions. The resemblance with those recorded for toluene-h_8 is obvious, with the maxima for the pump/ probe signals occurring at longer time delays.

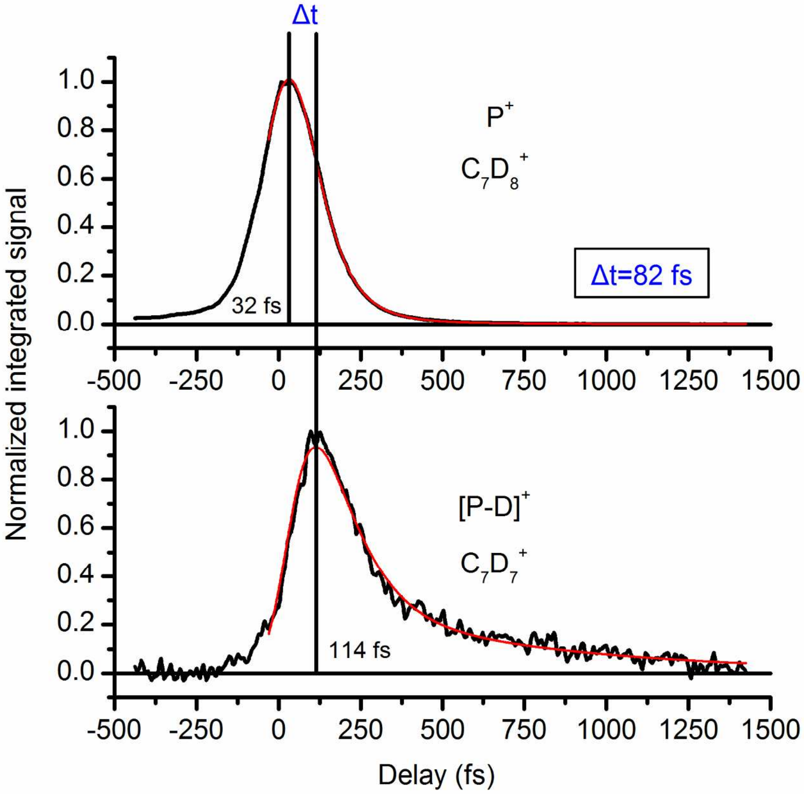

Fig. 3 Normalized sum of seven normalized scans for the case of toluene-d_8 (black lines). The fitting with eq. (6) (sup. information, red line) and the peak-signal positions are also shown.

3) Toluene-α,α,α-d_3

This partially deuterated derivative, having deuterium atoms only in the methyl group, was studied in order to elucidate the origin of the H- (or D-) elimination in h_8 (or d_8) analogues. Nevertheless, apart from the P^+ ($C_7H_5D_3^+$) ion (m/z=95), both the $[P-H]^+$ ($C_7H_4D_3^+$) and $[P-D]^+$ ($C_7H_5D_2^+$) ion fragments were observed (m/z=94 and 93) in the TOF spectra. We assigned the m/z=93 peak to the $[P-D]^+$ ion and not to a $[P-2H]^+$ ion, because no such a peak was observed in the cases of the other two molecules under the same experimental conditions.

In Fig. 4 the dynamics of these three ions is presented along with their maxima positions. It is clear that their time behavior differs from those recorded for the other two molecules.

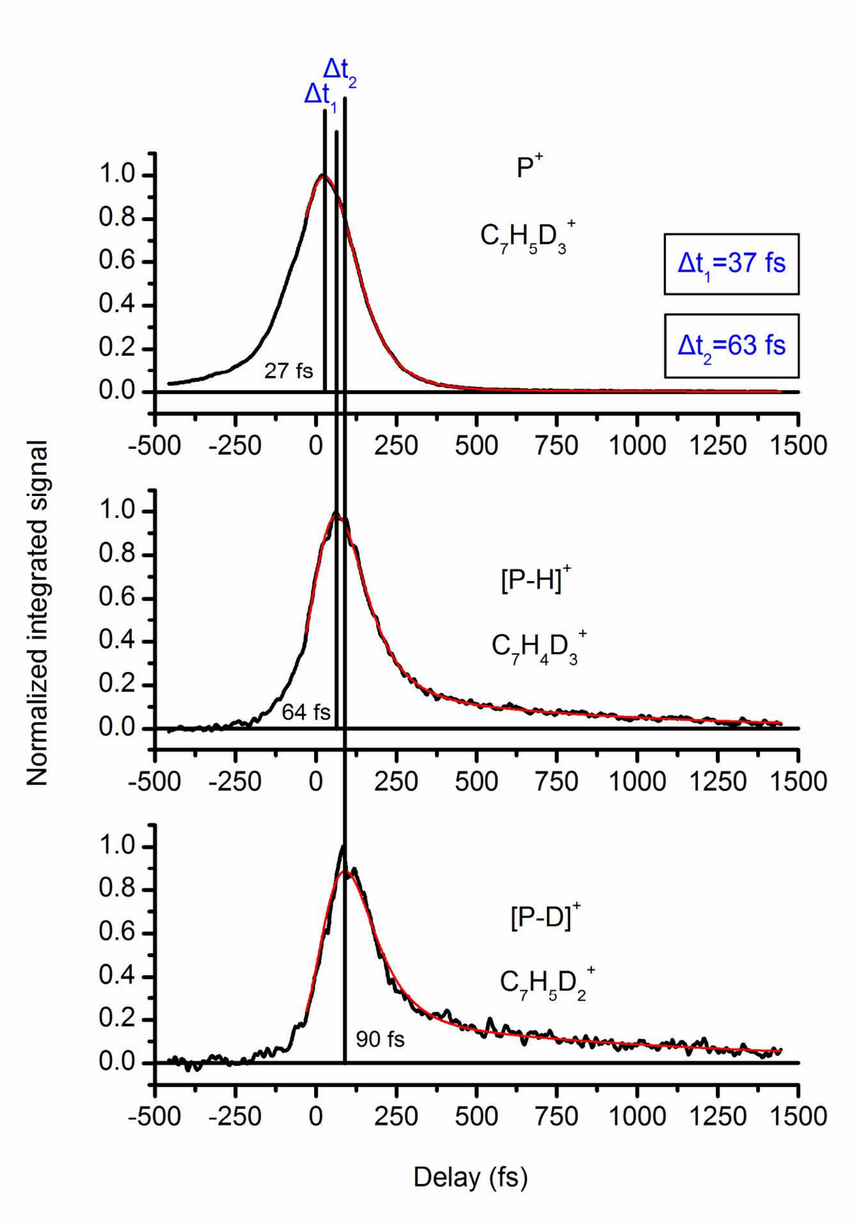

Fig. 4 Normalized sum of six normalized scans for the case of toluene-α,α,α-d$_3$ (black lines). The fitting with eq. (6) (sup. information, red line) and the peak-signal position are also shown.

In order to accurately determine the time behavior of the initially excited states, we utilized the rate equation model originally developed by W. Fuß and coworkers[25] in a fitting process applied on the parent and fragment ions time-dependent signals for all the three isotopomers. According to this model, the initially excited -by the pump pulse-population decays by passing through several locations L_n on the same PES or on different PESs of coupled excited states. The probe beam, which interacts with the decaying population after a time Δt, induces ionization and/or fragmentation. Each location is characterized by the lifetime τ_n and the ionization cross-section s_n, which depends on the specific features of the corresponding location and the number l of probe photons needed for ionization/fragmentation. Because of the statistical nature of the experiment, the total ion signal is the sum of the individual signals from each location and is described by a sum of exponentials convoluted with the instrumental function, that is the cross-correlation function between the pump pulse and the l-th power of the probe pulse. The instrumental function is derived by the H_2O^+ signal. (For a more detailed description of the fitting model, see the supporting information and ref. 25.) It should be mentioned that the model takes no account for the existence of branching during the decay process and for the possible initial excitation (by the pump beam) of more than one states. In these cases, the processes cannot be, in general, disentangled by using this specific model. An exception to the latter case exists when the initially excited states differ greatly concerning their lifetimes and cross-sections. Such a case will be discussed later in a following paragraph.

The ionization potential (IP) of toluene-h_8 is 8.828 eV,[26] while the appearance energy (AE) of the fragment ion is ~10.7 eV.[26] Therefore, for the P^+ and $[P\text{-}H]^+$ production, absorption of at least one and two probe photons is needed respectively, after the excitation by one pump photon. This indicates the values of the parameters that should be used in the fitting process along with the known probe pulse duration τ_{pr}, measured by a non-collinear single-shot autocorrelator, and the pump pulse duration, which is determined indirectly using the experimentally defined response function of the experimental setup (cross-correlation of the pump and probe beam measured in water, see supporting information). The same values were used for the deuterated compounds, for no significant difference in their IPs and AEs occurs.[20] In Figs. 2, 3 and 4 the fitted curves are also depicted (red lines). The resulting time constants τ_n and the corresponding cross-sections for ionization s_n are listed in Tables 1, 2 and 3 for toluene-h_8, toluene-d_8 and toluene-α,α,α-d_3 respectively.

Table 1 Time constants and corresponding cross-sections of the locations L_n for the case of toluene-h_8.

		Rydberg 4p	S_3	S_2	S_1
τ_n (fs)		690±50	76±10	55±10	560±50*
s_n	$C_7H_8^+$ (P^+)	0.0054±0.0005	0.93±0.09	0	0
s_n	$C_7H_7^+$ ($[P\text{-}H]^+$)	0	0	1.8±0.2	0.11±0.01

Table 2 Time constants and corresponding cross-sections of the locations L_n for the case of toluene-d_8.

		Rydberg 4p	S_3	S_2	S_1
τ_n (fs)		380±50	77±10	85±10	670±50*
s_n	$C_7D_8^+$ (P^+)	0.011±0.001	1.1±0.1	0	0
s_n	$C_7D_7^+$ ($[P\text{-}D]^+$)	0	0	1.3±0.1	0.13±0.01

Table 3 Time constants and corresponding cross-sections of the locations L_n for the case of toluene-α,α,α-d_3. Italics in τ_2 and τ_1 correspond to the decay times found for the $[P\text{-}D]^+$.

		Rydberg 4p	S_3	S_2	S_1
τ_n (fs)		450±50	78±10	27±10 *40±10*	710±50* *990±50**
s_n	$C_7H_5D_3^+$ (P^+)	0.011±0.001	0.93±0.09	0	0
s_n	$C_7H_7^+$ ($[P\text{-}H]^+$)	0	0	3.3±0.3	0.089±0.009
s_n	$C_7D_7^+$ ($[P\text{-}D]^+$)	0	0	2.2±0.2	0.11±0.01

*For the values corresponding to S_1 see the text.

The time behavior of the fragment ions differs greatly from that of the corresponding parent ions in all the three molecules. This strongly implies that they do not have the same origin as far as the neutral precursor is concerned, otherwise they would be proportional to each other.[27]

More specifically, in toluene-h_8 we have found two time constants for P^+ and three for $[P\text{-}H]^+$. For the P^+ a relatively short, at 76 fs (τ_3), and a long, at 690 fs (τ_R), have been determined. The τ_3 lifetime accounts also for the shift of the maximum of the transient signal by about 26 fs after the zero-point delay (Fig. 2). Spectroscopic studies on toluene-h_8 by Bolovinos *et al.*[6] proved the existence of two Rydberg states at 160.4 nm and 163.4 nm, both lying within the bandwidth of the pump pulse, built on the high-energy tail of the third excited valence state S_3 (corresponding to the $^1E_{1u}$ state of benzene), whose origin lies at ~188 nm (~6.6 eV).[28,29] They were assigned to 4p-Rydberg states. Their lifetimes, as estimated by the width of the corresponding spectral features, are expected to be similar. As a consequence, they cannot be distinguished by the fitting model. The spectral features imply also that the lifetime of the S_3 state is smaller than that of the Rydberg states by one order of magnitude. Thus, it is reasonable to assign the 76 fs lifetime to the S_3 valence state and the 690 fs to the Rydberg ones. The time dependence of the toluene ion has been reported previously under a similar excitation scheme,[4,30] while those for $[P\text{-}H]^+$ and the deuterated isotopomers are presented here for the first time. Our value τ_3=76±10 fs is also in reasonable agreement with the previously reported 100±30 fs (without any assignment) after excitation at 155 nm.[4] For toluene-d_8 and toluene-α,α,α-d_3 we have determined similar decay times (77±10 fs and 78±10 fs respectively).

The time constant τ_R=690±50 fs of toluene-h_8 is assigned to relaxation from the 4p-Rydberg states, as mentioned previously. Probably, this time characterizes the departure from the initially excited Rydberg states towards the S_3 valence state via a not easily accessible conical intersections (CIs), as observed for example in the case of ethylene.[31] The molecule would then leave much faster from S_3 (in τ_3). The respective decay times τ_R=380±50 fs and 450±50 fs for toluene-d_8 and toluene-α,α,α-d_3 are faster and with higher cross-sections, especially for the totally deuterated compound. These long times imply that the access to the CI requires an activation energy. In the deuterated molecules, the decrease of the zero-point energy, in particular in S_0, leads to the excitation of higher vibrational levels, closer to the barrier, by the pump photon, making thus the access to the CI easier and accelerating the process.

To be accurate, the contributions of the valence and the Rydberg states should have been disentangled by subtracting the Rydberg one from the total time-dependent P^+ signal before the application of the fitting model (which is applicable, as noted above, only to the cases where one initially excited state deactivates towards another one and so on). In fact, the P^+ signal in long times was fitted by a single exponential function, convoluted with the response function, extrapolated to negative times and then subtracted from the total signal. After this, the rate equation model was applied to the remaining signal. Nevertheless, we found that this process made actually no significant difference in the resulting decay times τ_R and τ_3 (within the error limits), because the two processes differ greatly both in time and cross-section.

As far as the $[P\text{-}H]^+$ dynamics is concerned, three time constants have been found, the first one (τ_3) with zero cross-section. This means that the S_3 valence state leads only to P^+ ions production after the interaction with the probe beam but not to $[P\text{-}H]^+$ fragment ions. This zero cross-section is responsible for the delayed peak position of the fragment with respect to the parent (Δt=69 fs). In other words, whereas τ_3 shows up in the P^+ signal as the decay time from S_3, it appears in the rising wing of the $[P\text{-}H]^+$, which is assigned to the S_2 state (see discussion on τ_2). This is a direct confirmation of the precursor-successor relationship: S_2 is populated from the decaying S_3. Zero cross-section is an indication that the excess energy is not sufficient for reaching the dissociation limit. Traeger and McLoughlin[10] found an appearance energy of 10.71 eV for $C_7H_7^+$, which can be reached only by two-probe-photon absorption in our case. However, Schwell and coworkers[32] give an onset value of 11.43 eV (three-probe-photon absorption needed), stating that the $C_7H_7^+$ signal was extremely low in the 10.71-11.4 eV region. In the scope that, as mentioned, our probe beam intensity was kept low, it seems reasonable that no fragment ions are observed from the S_3 valence state. The decay time of the S_3 state presents no difference for the deuterated compounds (77±10 fs and 78±10 fs for $C_6D_5CD_3$ and $C_6H_5CD_3$ respectively). In general, short times (<100 fs) imply a relaxation through an easily accessible CI. Apparently, the S_3 and S_2 surfaces intersect near the S_3 minimum. The fact that deuteration does not affect τ_3 means that their relative displacement and the relaxation happen along a coordinate with no significant H displacement but with deformation of the ring (possibly a C-C stretch in the π system).

The second time constant found from the $[P\text{-}H]^+$ transient signal is 55±10 fs (τ_2) for toluene-h_8 and increases to 85±10 fs for the totally deuterated analogue. This lifetime is assigned to the second excited valence state S_2 (corresponding to the $^1B_{1u}$ state of benzene, at ~5.8 eV[28,29]). Farmanara and coworkers[5] determined a time constant of 50±10 fs for the IC from the S_2 to the S_1 state, while Suzuki *et al.*[2] gave a lifetime of 62±4 fs, both in very good agreement with our value within the error limits. The fact that the cross-section for generation of fragment ions is now non-zero indicates the generation of hot parent ions from the highly-vibrationally excited S_2 state that undergo almost complete (zero-cross section for P^+) dissociation. As mentioned before, short lifetimes indicate the existence of easily accessible CIs. The increment of τ_2 observed upon complete deuteration (toluene-d_8) strongly implies that the reaction coordinate involves H displacement. A possible interpretation could be an out-of-plane "half-boat" deformation, similar to that calculated by Palmer *et al.*[33] for the case of the $S_2 \rightarrow S_1$ CI in benzene (prefulvene structure).

As far as the third lifetime τ_1 (560±50 fs for the tol-h_8 and 670±50 fs for the tol-d_8 compound) is concerned, we attribute it to relaxation from the S_1 state, with origin at ~4.6 eV.[28,29] In ref. 5 (excitation at 200 nm) it is estimated that this relaxation takes place at a much longer timescale (4.3±0.2 ps). The large deviation from the reported value is expected, since relaxation from S_1 occurs over a barrier, as implied by the long lifetimes (obviously in resemblance to "channel 3" in benzene), thus strongly depends on the excess energy. Therefore, the values presented in Tables 1-3 for the relaxation of the S_1 state are much lower with respect to those reported in ref. 5, but their estimation is useful in order to exclude the scenario that the long lifetimes, assigned as τ_1, characterize the Rydberg states. Although the τ_1 and τ_R could be considered as similar within the error limits for toluene-h_8, their behavior upon deuteration is totally different as can be easily observed in Tables 1, 2 and 3, leading thus to the conclusion that they do not have the same origin. Out-of-plane coordinates are probably involved on the $S_1 \rightarrow S_0$ path in analogy with the benzene case,[34] thus slower time constants are expected upon deutaration, which is in agreement with our observations.

Fig. 5 summarizes schematically the relaxation processes taking place.

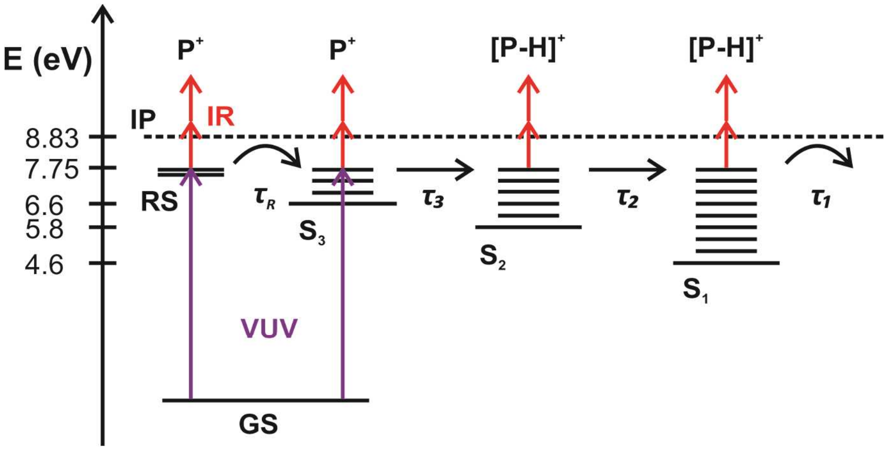

Fig. 5 Ionization scheme for toluene-h_8. Two 4p-Rydberg states and the S_3 valence state are excited by one VUV photon. Absorption of the IR beam leads only to P^+ ions from S_3 and the Rydberg states, while only $[P-H]^+$ ions are produced from S_2 and S_1, because for Franck-Condon reasons more probe photons are probably involved, leading thus to fragmentation. Bent arrows indicate the involvement of activation energy in the corresponding processes.

Another remarkable observation is that near the peak of the $[P-H]^+$ and $[P-D]^+$ time-dependent signals, small peaks with a time separation of about 30-40 fs appeared persistently. Fourier analysis of the signal in the 0-200 fs delay range has verified that there is a modulation with characteristic periods of 30±2 fs (1110±80 cm^{-1}) for $C_7H_7^+$, 36±3 fs (930±80 cm^{-1}) for $C_7D_7^+$, 40±4 fs and 41±6 fs (830±80 cm^{-1} and 800±100 cm^{-1}) for $C_7H_4D_3^+$ and $C_7H_5D_2^+$ released from toluene-α,α,α-d_3 respectively (the error is larger in the partially deuterated compounds due to the smaller signal-to-noise ratio). This modulation in the case of $C_7H_7^+$ originating from toluene-h_8 is presented in Fig. 6. These oscillations are evident for delay times up to ~200 fs in the present work. For longer delay times the peaks' amplitude decreases, following the trend of the $[P-H]^+$ ($[P-D]^+$) signal.

This observation can be attributed to wavepacket oscillations along the potential energy surface (PES) of the neutral precursors (variation of the ionization probability due to the Franck-Condon factor as the wavepacket moves on the PES). The fact that this modulation appears only in the fragment signals indicates that it does not take place in the S_3 or the Rydberg states. It is assigned hence to the S_2 excited state, because additionally it appears too early to belong to S_1. The oscillation is excited by a down-slope of the potential on entering S_2 and thus carries information on the relative shift of the S_2 versus S_3 PES and/or the CI between them.

The $C_7H_7^+$ signal shows a faster modulation than the other three isotopomers, which have almost the same period within the error limits. The fact that they are affected mainly by methyl deuteration makes it reasonable to assign them to vibrational modes related to the methyl group, either i) methyl-localized or ii) ring-deformative motion involving the methyl group. For the first case (i), from the IR and Raman spectra of toluene and the studied isotopomers it is known that the frequency values of the bending/rocking methyl-localized vibrations lie in the 1450-770 cm^{-1} range.[19,35–37] Following the Varsányi notation, these modes have been assigned as δ_{as}^{+}, δ_s and δ_{as}^{-}. The higher frequency values correspond to toluene-h_8, while for the methyl-deuterated isotopomers the corresponding values are almost identical. This trend is in agreement with our results within the experimental error. It should be noted that the abovementioned frequency values have been determined for the ground state (S_0). To the best of our knowledge, the frequency values of the δ_{as}^{+}, δ_s and δ_{as}^{-} modes in the S_2 state are not known, but at the excited electronic states they are expected to be reduced, as pointed out by theoretical calculations by Gardner *et al.*[37] for the S_1 case. For the latter case (ii), an out-of-plane bending involving the methyl group, such as the “half-boat” deformation, could be a possible assignment that would be also consistent with the discussion made before on the lifetime τ_2. As a consequence, we tend to consider this interpretation as the most consistent with all our observations.

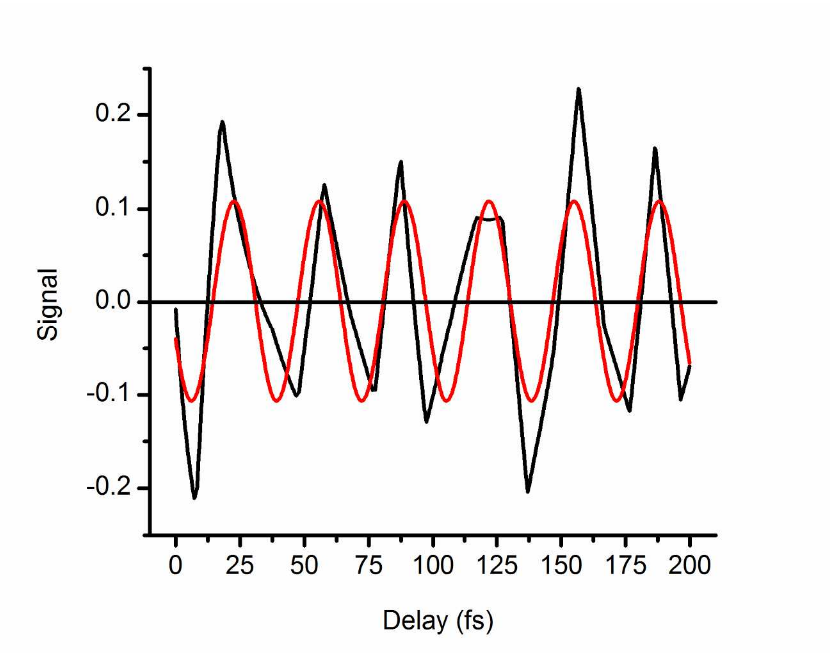

Fig. 6 Oscillations of the $C_7H_7^+$ signal in the 0-200 fs delay range. Experimental data after subtraction of the rate equation fitted curve (black line) along with the sinusoidal fitted curve (red line) on a typical run. Application of the same process on each run gives an average period of 30±2 fs (1110±80 cm^{-1}).

The case of the partially deuterated toluene ($C_6H_5CD_3$) is discussed separately, because it offers the possibility of studying simultaneously the H- and D-loss channels. Moreover, Davies and coworkers[38] have discussed extensively the role of doorway states in the acceleration of Internal Vibrational Redistribution (IVR) in toluene-h_8 and toluene-α,α,α-d_3 on the PES of S_1. Using ps time-resolved photoelectron imaging spectroscopy as a probe, they concluded that doorway states are critical in mediating the relaxation dynamics. The assigned combinations of vibronic states acting as doorway ones were different for the two compounds $C_6H_5CH_3$ and $C_6H_5CD_3$.

The decay times determined by the fitting process in the present work are listed in Table 3. It can be easily observed that the lifetime assigned to the Rydberg states lies between the corresponding values for the tol-h_8 and the tol-d_8 analogues. This is consistent with the consideration of higher vibrational states excitation in the deuterated compounds as discussed earlier. The decay time τ_3 is similar to those determined for the other two molecules.

The transient signals of the two different fragment ions $[P\text{-}H]^+$ and $[P\text{-}D]^+$ are of particular interest. First of all, the lifetimes assigned to the S_2 state appear slightly different for the two fragments (27±10 and 40±10 fs for $[P\text{-}H]^+$ and $[P\text{-}D]^+$ respectively). Although this differentiation could be considered as negligible within the error limits, it could also imply that there are two slightly different pathways on the S_2 PES, leading to H- or D-elimination after ionization. Furthermore, it is noteworthy that these two decay times are shorter than the corresponding τ_2 of $[P\text{-}H]^+$ in the case of toluene-h_8. Field and coworkers in one of their works[39] noticed that "the H- or D-loss in this species is easier than for the other two isotopic toluenes". Although they refer to the energy aspect, this could be also related to faster processes too.

The lifetimes assigned as τ_1 are also different for the two fragment ions of the partially deuterated compound. τ_1 determined from $[P\text{-}H]^+$ lies within the error limits of the corresponding value for the totally deuterated compound, while this determined from $[P\text{-}D]^+$ is certainly larger. The fact that τ_1 has a different value for the two fragments of toluene-d_3 (710±50 and 990±50 fs for $[P\text{-}H]^+$ and $[P\text{-}D]^+$ respectively) seems to support the assumption of the different pathways. This differentiation does not affect the fitting process on P^+, because the respective cross-sections are zero.

An interesting point, which have been discussed extensively in the past,[14,17,18,39,40] is that related to the relative abundance of the $[P\text{-}H]^+$ and $[P\text{-}D]^+$ ions or, in other words, the comparison between the H- and D-loss dissociation channels. Three different processes can take place in the ion of toluene-α,α,α-d_3: 1) H-loss from the ring, 2) D-loss from the methyl group and 3) scrambling. The effect of the position of the H- or D-atom is described by the preference factor, which in general favors the loss from the methyl group, while that of the deuteration by the isotopic factor, which favors the H-loss. Howe and McLafferty[40] concluded that both the deuterium isotope effect and the degree of scrambling decrease with increasing the internal energy of the ion. Lifshitz *et al.*[14,15] report also on the decrease of the H/D-loss ratio on the photon energy using the time-resolved photoionization mass spectrometry (TPIMS) technique. According to Field *et al.*,[39] who have determined the AE for the H- and D-loss channels using synchrotron radiation, the AE for H-loss for toluene-α,α,α-d_3 is lower than that for toluene-h_8. Furthermore, they found that it is easier to remove a H-atom originally located on the aromatic ring than a D-atom originally being on the methyl group. In order to clarify whether a deuterium isotope or a position preference effect is on operation, they measured the ratio R=[-H]/[-D] as a function of the ionic internal energy. They estimated it at ~2.03 over the excitation energy range from 25 to 100 eV, i.e. higher than that implied by the molecular stoichiometry (5/3=1.67). They concluded hence that the isotope effect, possibly in combination with atom scrambling, is dominant. All the above mentioned works examined also the possibility of isomerization of the six-membered ring structure of the cation to a seven-membered ring structure separately or in combination with the three other processes and they found that it is not negligible.

In Fig. 7 we present the ratio R as a function of the delay time. It is obvious that the H-loss channel dominates in short timescales. Moreover, it is clear that the ratio R strongly depends on the delay time and decreases as it increases. At zero-delay time the ratio is ~5, but for longer delay times (in the order of ps), it seems to reach the determined by Field *et al*. value, i.e. the stoichiometric value affected by the isotope factor and the scrambling. This trend looks very similar to the dependence of these two effects on the internal energy of the ion. More specifically, the value 5 at zero-delay corresponds to an internal energy of ~12 eV in ref. 14, which could be reached by one pump and three probe photons in our experiment. As the delay between the two beams increases and the wavepacket of the excited molecules move down along the PESs, the excess energy increases, leading thus to the production of hotter ions after the interaction with the probe beam. This strongly implies that the vibrational energy plays the key role in the processes involved. The increase of the vibrational energy could be related to excitation of modes associated with motion of the methyl group. This would favor the D- over the H-loss, leading to the decrease of the ratio R. This is consistent with the discussion about the observed oscillations made above and with the statement made by Lifshitz[15] that “the steep rise of the isotope effect at low photon energies reflects a broadening effect of the thermal energy distribution”.

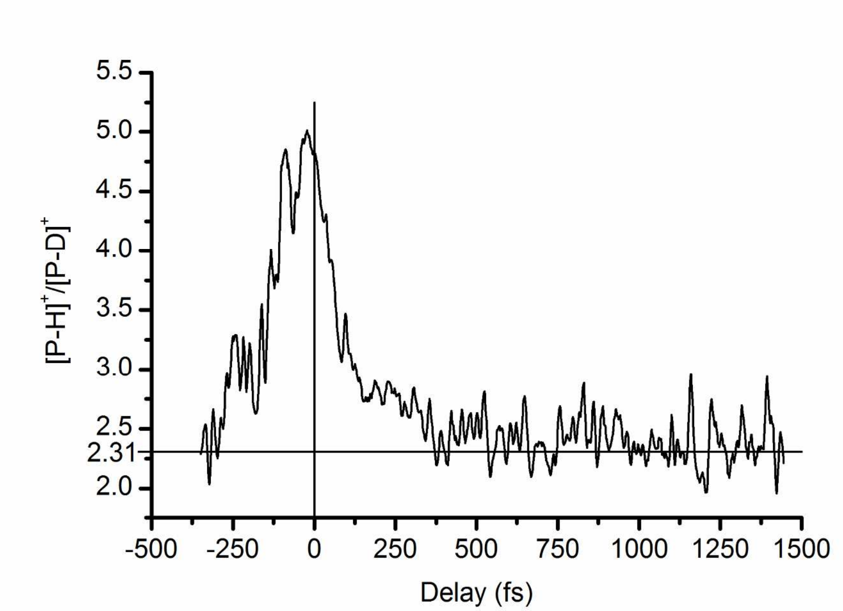

Fig. 7 $[P\text{-}H]^+/[P\text{-}D]^+$ ratio for the case of toluene-α,α,α-d_3. At long delay times it tends to reach the stoichiometric value affected by the isotope effect in combination with scrambling (see text).

Another possible interpretation of the $[P\text{-}H]^+/[P\text{-}D]^+$ ratio behavior could be the isomerization of the ionic six- to a seven-membered ring structure (cycloheptatriene) in the acceleration region of the TOF. This process is known to exhibit activation energy, which can be reached more easily as the neutral precursors obtain more excess energy, i.e. as the delay increases. The seven-membered structure could favor the loss of an atom originally located in the methyl group, that is a D atom in the case of toluene-α,α,α-d_3. In any case, cycloheptatriene has been found to present close similarities to toluene concerning the isotope effect and scrambling[40] and hence the involvement of this structure cannot be excluded by our discussion.

The same H/D-loss processes are obviously involved in toluene-h_8 and toluene-d_8 too, but in these cases the lack of labelling makes them impossible to be investigated by using the TOFMS technique.

Conclusions

Our studies on three isotopologues of toluene, i.e. toluene-h_8, toluene-d_8 and toluene-α,α,α-d_3, have elucidated the temporal behavior of the parent and of the corresponding fragment -after H- or D-elimination- ions in the femtosecond timescale by utilizing the VUV pump-IR-probe technique. Two superimposed processes have been observed: i) the decay from the 4p-Rydberg states to the S_3 valence state, which is affected by deuteration and takes place over a barrier, and ii) the relaxation of S_3 to the energetically lower-lying S_2 valence state, with the same time constants for all the molecules studied implying the existence of an easily accessible CI. A wavepacket oscillation on the S_2 PES is manifested from the analysis of the dynamics of the fragment ion signals. The corresponding frequencies could be attributed to out-of-plane vibrations involving also the methyl group, since they are affected by deuteration. These findings are in agreement with the structure described previously for the analogous CI in the benzene molecule.

As far as the H- and D-loss channels are concerned, from the partially deuterated toluene data analysis we concluded that their ratio is time-depended. The isotope effect and scrambling dependence on the excess energy seems to be responsible for the time behavior, while the isomerization of the ion to a seven-membered structure cannot be excluded.

Experiments using laser sources of variable wavelength, for example Optical Parametric Amplifiers (OPAs), for both the pump and the probe beam are planned to be performed in the future. They are expected to give further information on the processes and states involved by selecting specific excited states.

Acknowledgments

The authors would like to thank Asst. Prof. E. P. Benis for his contribution in the development of the experimental setup as well as Dr. W. Fuß and coworkers for the useful discussion and for providing the fitting code. The experiments were performed in the Central Laser Facility of the University of Ioannina. This research has been co-financed by the European Union (European Social Fund - ESF) and Greek national funds through the Operational Program “Education and Lifelong Learning” of the National Strategic Reference Framework (NSRF) – Research Funding Program: **THALES (ISEPUMA)**, Investing in knowledge society through the ESF.

References

1 W. Radloff, V. Stert, T. Freudenberg, I. V. Hertel, C. Jouvet, C. Dedonder-Lardeux and D. Solgadi, *Chem. Phys. Lett.*, 1997, **281**, 20–26.
2 Y.-I. Suzuki, T. Horio, T. Fuji and T. Suzuki, *J. Chem. Phys.*, 2011, **134**, 184313.
3 Y. Kajii, K. Obi, I. Tanaka, N. Ikeda, N. Nakashima and K. Yoshihara, *J. Chem. Phys.*, 1987, **86**, 6115–6118.
4 P. Farmanara, O. Steinkellner, M. T. Wick, M. Wittmann, G. Korn, V. Stert and W. Radloff, *J. Chem. Phys.*, 1999, **111**, 6264–6270.
5 P. Farmanara, V. Stert, W. Radloff and I. V. Hertel, *J. Phys. Chem. A*, 2001, **105**, 5613–5617.
6 A. Bolovinos, J. Philis, E. Pantos, P. Tsekeris and G. Andritsopoulos, *J. Chem. Phys.*, 1981, **75**, 4343–4349.
7 M. Vacher, D. Mendive-Tapia, M. J. Bearpark and M. A. Robb, *J. Chem. Phys.*, 2015, **142**, 094105.
8 M. Vacher, J. Meisner, D. Mendive-Tapia, M. J. Bearpark and M. A. Robb, *J. Phys. Chem. A*, 2015, **119**, 5165–5172.
9 S. Cogan, Y. Haas and S. Zilberg, *J. Photochem. Photobiol. Chem.*, 2007, **190**, 200–206.
10 J. C. Traeger and R. G. McLoughlin, *Int. J. Mass Spectrom. Ion Phys.*, 1978, **27**, 319–333.
11 J. H. Moon, J. C. Choe and M. S. Kim, *J. Phys. Chem. A*, 2000, **104**, 458–463.
12 F.-S. Huang and R. C. Dunbar, *Int. J. Mass Spectrom. Ion Process.*, 1991, **109**, 151–170.
13 C. Lifshitz, Y. Gotkis, A. Ioffe, J. Laskin and S. Shaik, *Int. J. Mass Spectrom. Ion Process.*, 1993, **125**, R7–R11.
14 C. Lifshitz, Y. Gotkis, J. Laskin, A. Ioffe and S. Shaik, *J. Phys. Chem.*, 1993, **97**, 12291–12295.
15 C. Lifshitz, *Acc. Chem. Res.*, 1994, **27**, 138–144.
16 C.-K. Lin, C.-L. Huang, J.-C. Jiang, A. H. H. Chang, Y. T. Lee, S. H. Lin and C.-K. Ni, *J. Am. Chem. Soc.*, 2002, **124**, 4068–4075.
17 J. H. Beynon, J. E. Corn, W. E. Baitinger, R. M. Caprioli and R. A. Benkeser, *Org. Mass Spectrom.*, 1970, **3**, 1371–1377.
18 M. Bertrand, J. H. Beynon and R. G. Cooks, *Org. Mass Spectrom.*, 1973, **7**, 193–201.
19 W. J. Balfour and Y. Fried, *Can. J. Phys.*, 1994, **72**, 1218–1224.
20 W. J. Balfour and R. S. Ram, *Can. J. Phys.*, 1994, **72**, 1225–1235.
21 P. B. Corkum, *Phys. Rev. Lett.*, 1993, **71**, 1994–1997.
22 M. Lewenstein, P. Balcou, M. Y. Ivanov, A. L'Huillier and P. B. Corkum, *Phys. Rev. A*, 1994, **49**, 2117–2132.
23 K. Kosma, S. A. Trushin, W. E. Schmid and W. Fuss, *Opt. Lett.*, 2008, **33**, 723–725.
24 S. A. Trushin, W. E. Schmid and W. Fuß, *Chem. Phys. Lett.*, 2009, **468**, 9–13.
25 K. Kosma, Ph.D. Thesis, Ludwig-Maximilians-Universität München, 2008.
26 *NIST Chem. WebBook*, http://webbook.nist.gov/chemistry/, (accessed May 2015).
27 S. A. Trushin, S. Diemer, W. Fuß, K. L. Kompa and W. E. Schmid, *Phys. Chem. Chem. Phys.*, 1999, **1**, 1431–1440.

28 Photoelectric Spectrometry Group and Institut für Spektrochemie und Angewandte Spektroskopie, *UV atlas of organic compounds*, Butterworth, London, 1966, vol. II.
29 G. Cucchiara, R. Dovesi, F. Ricca and L. Cerruti, *J. Mol. Struct.*, 1978, **43**, 61–74.
30 M. Wittmann, M. T. Wick, O. Steinkellner, P. Farmanara, V. Stert, W. Radloff, G. Korn and I. V. Hertel, *Opt. Commun.*, 2000, **173**, 323–331.
31 K. Kosma, S. A. Trushin, W. Fuß and W. E. Schmid, *J. Phys. Chem. A*, 2008, **112**, 7514–7529.
32 M. Schwell, F. Dulieu, C. Gée, H.-W. Jochims, J.-L. Chotin, H. Baumgärtel and S. Leach, *Chem. Phys.*, 2000, **260**, 261–279.
33 I. J. Palmer, I. N. Ragazos, F. Bernardi, M. Olivucci and M. A. Robb, *J. Am. Chem. Soc.*, 1993, **115**, 673–682.
34 B. R. Smith, M. J. Bearpark, M. A. Robb, F. Bernardi and M. Olivucci, *Chem. Phys. Lett.*, 1995, **242**, 27–32.
35 J. K. Wilmshurst and H. J. Bernstein, *Can. J. Chem.*, 1957, **35**, 911–925.
36 G. Varsanyi, *Assignment for vibrational spectra of seven hundred benzene derivatives*, Adam Hilger, London, 1974, vol. 1.
37 A. M. Gardner, A. M. Green, V. M. Tamé-Reyes, V. H. K. Wilton and T. G. Wright, *J. Chem. Phys.*, 2013, **138**, 134303.
38 J. A. Davies, A. M. Green, A. M. Gardner, C. D. Withers, T. G. Wright and K. L. Reid, *Phys. Chem. Chem. Phys.*, 2014, **16**, 430–443.
39 T. A. Field, F. Dulieu, J.-H. Fillion, J.-L. Chotin, S. Douin, J.-L. Lemaire and S. Leach, *Chem. Phys.*, 1999, **250**, 81–110.
40 I. Howe and F. W. McLafferty, *J. Am. Chem. Soc.*, 1971, **93**, 99–105.